Prediction of turbulent source flow between stationary and rotating discs

C. R. Truman* and D. F. Jankowski†

Results are presented from a numerical investigation of turbulent source flow between two discs, both of which are stationary or corotating. Parabolic flow was assumed and the Box Method used to obtain marching solutions of the governing equations. Turbulence modelling was based on extensions of classical eddy-viscosity/mixing-length concepts which reflect the influences of divergence of the mean-flow streamlines and non-isotropic Reynolds stresses due to disc rotation. The predictions for the rotating case are the first local results available. For the stationary case, earlier work has been extended by the use of empirical formulae for reverse transition and inclusion of the influence of streamline divergence. Comparisons with limited data for stationary and corotating discs show reasonable agreement. Although the turbulence models are probably not optimum, they provide an adequate basis for engineering studies of turbulent source flow between corotating and stationary discs until more extensive and reliable empirical information is available

Keywords: *turbulence, modelling, corotating discs, stationary discs, source flow*

Turbulent source flow between stationary or corotating parallel discs occurs in such practical applications as the manufacture of silicon chips[1] and the flow modelling for a computer-memory disc pack[2,3]. Less exotic, but still interesting, applications are diffusers and multiple-disc pumps[4].

Source flow between parallel discs also has intrinsic importance as an example of a 'complex turbulent flow'[5] in which the effects of rotation and streamline divergence play an important role. Progress in tubulence modelling has been such that it is now reasonable to attempt predictions for such flows. Turbulence models ultimately depend on experimental results. Since such information is frequently unavailable, a complex flow which is a perturbation of a classical thin shear layer is often considered (at least, in a first attempt) within the framework of a suitable extension of a thin-shear-layer turbulence model. Practical necessity and the expectation that useful ideas can be extracted from the substantial base of information and experience derived from thin-shear-layer studies over the past 80 years are the rationale behind such a treatment.

Various phenomena occur in turbulent source flow between stationary or corotating discs. Depending on the values of the flow parameters, laminar or turbulent flow, reverse transition, flow reversal and both inlet and exit separation are observed. The possibility of separation or flow reversal is neglected in this analysis which uses the thin-shear-layer equations for axisymmetric flow with or without rotation-induced swirl. Any elliptic regions near the entrance or exit of the flow region are assumed to comprise only a small part of the total region of interest. Flow reversal can also occur in the interior of the flow region for sufficiently large radius (or rotation rate); for radii beyond this initiation of reverse flow, the flow must be treated as elliptic.

Typically, small disc spacings are of practical interest so the effect of shear is important across the entire axial extent of the flow. Thus the flow must be modelled as an internal thin shear layer. This approximation ensures that the flow is parabolic in the radial direction and requires that the radial pressure-gradient be determined during a numerical marching process. Since the flow is assumed to be independent of the azimuthal coordinate in both the rotating and stationary cases, there are only two independent variables. While several suitable numerical methods are available, progress for the turbulent case has been hindered by the lack of a firm experimental base. However, concepts in turbulence modelling have now developed to the point where it is reasonable to expect useful information will result if turbulent source flow between parallel discs is treated as a perturbation of a classical thin shear layer with the additional effects of divergence of the mean-flow streamlines and non-isotropy of the turbulent stresses due to disc rotation.

An accurate finite-difference method exists for the determination of the laminar solution for (parabolic) radial flow between stationary or rotating discs[6]. The predictions for laminar radial flow with disc rotation were verified by Adams and Rice[7] and Pater, Crowther and Rice[8] by flow visualisation and measurement of the radial distribution of static pressure. Pater *et al*[8] also identified the region (in an appropriate parameter space) in which turbulent flow would be encountered. The related problem of reverse transition has been discussed, for

* Department of Mechanical Engineering, University of New Mexico, Albuquerque, New Mexico 87131, USA
† Department of Mechanical and Aerospace Engineering, Arizona State University, Tempe, Arizona 85287, USA
Received 23 July 1984 and accepted for publication in final form on 22 October 1984

stationary discs, by Narasimha and Sreenivasan[9]. Local (finite-difference) turbulent solutions for stationary discs have been provided by Bayley and Owen[10] for source flow and by Murphy, Chambers and McEligot[11] for sink flow. In both cases, simple eddy-viscosity turbulence models were used. Bayley and Owen also predicted the source flow between a stationary disc and a rotating disc with a turbulence model based on an isotropic mixing length, but non-isotropic eddy viscosities. There are no other local analyses of turbulent source, or sink, flow which include non-isotropic effects cause by disc rotation.

Measurements for turbulent flow between stationary discs include the axial distribution of the radial velocity at the exit radius, obtained using a pitot tube,[10,12] and axial distributions of radial velocity and turbulence intensity obtained with a hot-wire anemometer[13]. Agreement between these measurements and the available predictions is, at best, fair. This appears to be due partly to the occurrence of reverse transition.

For rotating discs, Bakke, Kreider and Kreith[13] performed a series of hot-wire measurements including radial and tangential velocity profiles and turbulence intensities. The reliability of these measurements is somewhat questionable and a detailed discussion is provided

Notation

A^+	Empirical constant in turbulence models, 26.0
c	Empirical constant in reverse-transition intermittency, Eq (16)
D_x, D	van Driest damping, Eqs (13) and (15)
F	Dimensionless stream function, Eq (8)
h	Spacing between the discs ($\ll r_s$)
l_x, l_{xo}	Mixing lengths, Eqs (11) and (14)
p	Time-averaged pressure
P	Dimensionless pressure, $p/(\rho\nu Q Re_s/2\pi h^3)$
P_o	Dimensionless pressure at exit of discs
Q	Volume flow rate between the discs
r, θ, z	Cylindrical coordinates
r_s	Starting radius
R	Dimensionless radial coordinate, $r/(Qh/2\pi\nu Re_s)^{1/2}$
R_s	Dimensionless starting radius, $(Re_s/Re_Q)^{1/2}$
Re	Local Reynolds number, $Q/\pi r\nu$
Re_Q	Throughflow Reynolds number, $Qh/2\pi\nu r_s^2$
Re_s	Scaling Reynolds number: Re_ω for $Re_\omega \geqslant 1$, 1 for $Re_\omega \leqslant 1$
Re_ω	Rotational Reynolds number, $\omega h^2/\nu$
S, T	Dimensionless viscous-stress components, Eq (17)
u, v, w	Time-averaged velocity components in r, θ, z directions
u', v', w'	Fluctuating velocity components in r, θ, z directions
U	Dimensionless radial velocity component, $u/(Q/2\pi hr)$
V	Dimensionless trangential velocity component, $v/\omega r$
W	Dimensionless axial velocity component, $w/[(Q\nu/2\pi h)^{1/2}/r]$
U', V', W'	Dimensionless fluctuating velocity components, $(u', v', w')/[(Q/2\pi h\nu)^{1/4} Re_s^{1/2}(\nu/h)]$
$-\overline{U'W'}$, $-\overline{V'W'}$	Dimensionless Reynolds stresses
z^*	Scale for z, $h/Re_s^{1/2}$
z^+	Dimensionless axial coordinate in van Driest damping, $z(\tau_w/\rho)^{1/2}/\nu$
Z	Dimensionless axial coordinate, z/z^*
Z_c	Dimensionless axial location of plane of symmetry, $Re_s^{1/2}/2$
$\frac{\partial u_t}{\partial z}$	Magnitude of velocity-gradient vector, $\left[\left(\frac{\partial u}{\partial z}\right)^2+\left(\frac{\partial v}{\partial z}\right)^2\right]^{1/2}$
α	Empirical constant in turbulence models, 10.0
γ	Intermittency for reverse transition, Eq (16)
ε_x	Eddy viscosity, Eq (10)
ε_R^+	Dimensionless radial eddy viscosity, ε_r/ν
ε_θ^+	Dimensionless tangential eddy viscosity, ε_θ/ν
κ	Empirical constant in turbulence models, 0.40
λ	Empirical constant in turbulence models, 0.12
ν	Kinematic viscosity of fluid
ρ	Fluid density
$-\rho\overline{u'w'}$, $-\rho\overline{v'w'}$	Reynolds stresses
τ_x	Shear-stress component in x direction
τ_x^+	Dimensionless shear-stress component in x direction, τ_x/τ_{xw}
τ_r	Radial shear stress, $\rho\nu\frac{\partial u}{\partial z}-\rho\overline{u'w'}$
τ_θ	Tangential shear stress, $\rho\nu\frac{\partial v}{\partial z}-\rho\overline{v'w'}$
τ	Magnitude of shear-stress vector, $(\tau_r^2+\tau_\theta^2)^{1/2}$
τ^+	Dimensionless magnitude of shear-stress vector, τ/τ_w
ω	Angular speed of the discs

Subscripts

cr	Value at beginning of reverse transition
lam	Value at end of reverse transition
w	Value at wall ($Z=0$)
x	Radial (r) or tangential (θ) component

Superscripts

prime (′)	Differentiation with respect to Z

later. The limitations of the available experimental evidence are, of course, a serious deterrent to the development of a reliable turbulence model.

Our work is concerned with a numerical investigation of turbulent source flow of an incompressible fluid between stationary and corotating discs. The flow parameters and geometry are assumed to be such that the axisymmetric parabolic-flow model is appropriate. In view of the limitations of the available experimental data, turbulence modelling was based on two extensions of classical eddy-viscosity/mixing-length concepts. These include Bradshaw's modification[5] of the mixing length to account for the extra strain rate due to streamline divergence and modifications to reflect the presence of rotation-induced, non-isotropic radial and tangential Reynolds stresses[14]. The effects of reverse transition were treated, where necessary, by an empirical correlation. The Box method[15] was used to obtain numerical solutions of the governing system of partial differential equations. Results for the turbulence models are compared to each other and, where appropriate, to experimental evidence. Reasons are suggested to explain the nature of the comparison.

Mathematical problem

The governing equations for turbulent source flow between stationary or rotating discs are obtained by applying scaling arguments to the incompressible, time-averaged Navier–Stokes system. These arguments embody the well-known thin-shear-layer approximation[5] so that only a suitable turbulence model need be added. With no dependence on the azimuthal coordinate θ, the approximate governing equations are:

$$\frac{\partial u}{\partial r}+\frac{u}{r}+\frac{\partial w}{\partial z}=0 \tag{1}$$

$$u\frac{\partial u}{\partial r}+w\frac{\partial u}{\partial z}-\frac{v^2}{r}=-\frac{1}{\rho}\frac{dp}{dr}+\nu\frac{\partial^2 u}{\partial z^2}-\frac{\partial \overline{u'w'}}{\partial z} \tag{2}$$

$$u\frac{\partial v}{\partial r}+w\frac{\partial v}{\partial z}+\frac{uv}{r}=\nu\frac{\partial^2 v}{\partial z^2}-\frac{\partial \overline{v'w'}}{\partial z} \tag{3}$$

It is convenient, for efficient numerical solution, to express Eqs (1)–(3) in terms of dimensionless variables scaled to be approximately unity in the region of interest. The choices of this scaling are motivated[16] by the balances already used to obtain the approximate equations and by the work of Boyd and Rice[6] and Murphy *et al*[11]. The only complication is the change in the relative importance of centrifugal acceleration in Eq (2) between the cases of stationary and rotating discs. It is simple to express Eqs (1)–(3) in terms of the new variables:

$$\frac{\partial U}{\partial R}+\frac{\partial W}{\partial Z}=0 \tag{4}$$

$$U\frac{\partial U}{\partial R}-\frac{U^2}{R}+W\frac{\partial U}{\partial Z}-\left(\frac{Re_\omega}{Re_s}\right)^2 R^3V^2 = -R^2\frac{dP}{dR}+R\frac{\partial^2 U}{\partial Z^2}+R^2\frac{\partial}{\partial Z}(-\overline{U'W'}) \tag{5}$$

$$U\frac{\partial V}{\partial R}+W\frac{\partial V}{\partial Z}+\frac{2UV}{R}=R\frac{\partial^2 V}{\partial Z^2}+\frac{Re_s}{Re_\omega}\frac{\partial}{\partial Z}(-\overline{V'W'}) \tag{6}$$

The scaled system contains a Reynolds number Re_Q to characterize the throughflow between the discs, and a Reynolds number Re_ω to reflect the influence of disc rotation. The 'scaling' Reynolds number Re_s arises because of the changing influence of centrifugal acceleration, as reflected in the axial-length scale z^*. When the radial inertial terms dominate, $z^*=h$ but when centrifugal acceleration is important, $z^*=(\nu/\omega)^{1/2}$, which can be interpreted as an Ekman-layer thickness. Use of Re_s allows both scales to be included in a single formula for z^*.

If the necessary boundary and starting conditions are added, the completed problem is suitable for a numerical solution. A solution is sought in an open sector of the R–Z plane which is described by $R\geqslant R_s$ and $0\leqslant Z\leqslant Z_c$. The starting conditions reflect the coupling between the inlet region where a set of elliptic equations govern and the parabolic-solution region. Thus it is impossible to determine 'exact' starting conditions without solving the elliptic inlet-region problem. This is not practical and defeats the purpose of making the thin-shear-layer approximation to obtain a parabolic system. The specification of starting conditions must then be somewhat arbitrary, but this is not significant since their influence should decay rapidly as R increases. No experimental information is available from which to determine these conditions. A convenient way to establish the starting conditions numerically is the concept of 'local similarity'[17] which will be discussed later since the chosen numerical-solution method requires additional starting information over that needed for Eqs (4)–(6).

The condition used to solve for dP/dR at each radial station is an integral version of conservation of mass, ie, for $R\geqslant R_s$:

$$\int_0^{Z_c} U(R,Z)\,dZ=Z_c \tag{7}$$

Numerical integration can be avoided if a stream function $F(R,Z)$ defined by:

$$U=\frac{\partial F}{\partial Z}\qquad W=-\frac{\partial F}{\partial R} \tag{8}$$

is introduced since Eq (7) then reduces to:

$$F(R,Z_c)-F(R,0)=Z_c \tag{9}$$

Moreover Eq (4) is automatically satisfied by the use of a stream function. A set of equations for F and V can be obtained by using the definitions of Eq (8) in Eqs (5) and (6). Finally the boundary conditions require no-slip and no penetration at $Z=0$ and symmetry at $Z=Z_c$ for $R\geqslant R_s$.

Turbulence modelling

For the problem of interest, the available experimental information is inadequate to support the adoption of a 'sophisticated' turbulence model. Hence heuristic arguments and broad comparisons with related work are the only available avenue for the development of models for $-\overline{U'W'}$ and $-\overline{V'W'}$. Such ideas led to the philosophy of treating these terms by extending classical mixing-length/eddy-viscosity concepts. The results should be adequate for engineering studies of parabolic turbulent flows between parallel discs.

Introduction of an eddy viscosity is common in the study of classical thin shear layers. Extensions of a mixing-length turbulence model have been successful in a variety of problems. In fact, for some flows, the more elaborate $k-\varepsilon$ model does not provide significantly better predictions than an extended mixing-length model. Examples include the boundary layer on a spinning cone[18] and flow over a single rotating disc[19]. This success is encouraging with regard to our decision to extend the mixing-length model here.

The presence of two important Reynolds stresses means that the usual definition for the eddy viscosity is inadequate. The first extension of the classical mixing-length model defines two eddy viscosities ε_r and ε_θ:

$$-\overline{u'w'}=\varepsilon_r\frac{\partial u}{\partial z} \tag{10a}$$

$$-\overline{v'w'}=\varepsilon_\theta\frac{\partial v}{\partial z} \tag{10b}$$

The notation is that of Eqs (1) to (3). While there have been successes[20,21] with an isotropic model ($\varepsilon_r=\varepsilon_\theta$), arguments in favour of anisotropic models for flows with rotation can be made[14,22]. Thus an anisotropic model based on a proposal by Koosinlin and Lockwood[14] is used. For $x=r$ or θ, a mixing length l_x is defined by:

$$\varepsilon_x=l_x^2\left[\left(\frac{\partial u}{\partial z}\right)^2+\left(\frac{\partial v}{\partial z}\right)^2\right]^{1/2}=l_x^2\frac{\partial u_t}{\partial z} \tag{11}$$

and the distribution of l_x is:

$$l_x=\begin{cases}\kappa z D_x & \kappa z\leqslant\dfrac{\lambda h}{2}\\[2ex] \dfrac{\lambda h}{2}, & \kappa z\geqslant\dfrac{\lambda h}{2}\end{cases} \tag{12}$$

where D_x is a version of the familiar van Driest damping:

$$D_x=1-\exp\left[\frac{-z^+(\tau_x^+)^{1/2}}{A^+}\right]. \tag{13}$$

The characteristic length for l_x was chosen as $h/2$ in accordance with previous work on stationary discs[10]. This model is anisotropic only in the wall layer where the damping functions D_r and D_θ are employed. Non-isotropic effects induced by rotation are expected to have greatest influence in this region.

The turbulence modelling must also reflect the extra strain rate associated with the streamline divergence caused by the radial increase of flow area. Bradshaw's hypothesis[5] that an increase in the mixing length should result has been verified experimentally for axisymmetric flow over a cone[23]. For the present problem, his proposal for a simple modification to model this increase takes the form:

$$\frac{l_x}{l_{xo}}=1+\alpha\left(\frac{u/r}{\partial u_t/\partial z}\right) \tag{14}$$

where l_{xo} is the mixing length from Eq (12), u/r is the extra strain rate and α is an empirical constant. Following Bradshaw, the magnitude of the 'correction' is limited by:

$$\left|\frac{u/r}{\partial u_t/\partial z}\right|\leqslant 0.1$$

This restriction is introduced due to the limited range over which the linear expression, Eq (14), can be expected to hold; it also ensures a finite mixing length at $Z=Z_c$ where $\partial u_t/\partial z=0$ due to the symmetry boundary conditions.

Four empirical constants (A^+, κ, λ, α) appear in Eqs (11)–(14). The constants A^+ and κ are given the widely used values, $A^+=26$ and $\kappa=0.4$. However, reported values for λ show a dependence on the flow situation[24]. For plane wall layers which have an inviscid outer flow, λ is typically 0.07 to 0.09 while for a parallel-plate duct in which wall layers merge at the duct centre line, experiments[25] found λ ranged from 0.10 to 0.15, with the higher value associated with merged wall layers; $\lambda=0.14$ can be predicted from the work of Cebeci and Chang[26]. Due to the presence of merged wall layers in source flow between parallel discs, λ was chosen as the mid-range value of 0.12. The remaining constant was given the value $\alpha=10$ in accordance with Bradshaw's recommendation. The sensitivity of the predictions to these choices is discussed later.

The anisotropic turbulence model defined by Eqs (10)–(13) will be referred to subsequently as tma. Another anisotropic model based on a suggestion by Rotta[27] was also implemented, but the results were less satisfactory than those obtained with tma[16]. An isotropic model, denoted by tmi, was also considered. Such a model has $\varepsilon_r=\varepsilon_\theta$ so that $l_r=l_\theta$ and hence $D_r=D_\theta$. Thus tmi need only replace Eq (13) by:

$$D=1-\exp\left[\frac{-z^+(\tau^+)^{1/2}}{A^+}\right] \tag{15}$$

The Bradshaw modification[14] was retained in tmi as were the chosen values for the empirical constants.

A detailed examination of the experimental results for source flow between stationary discs suggests the occurrence of reverse transition[9] in certain cases. This phenomenon cannot be predicted with tma or tmi and, in fact, there is no fundamental theory upon which to base a prediction method for reverse transition. Narasimha and Sreenivasan[9] suggested, as a working definition, that reverse transition has occurred when the mean-velocity distributions may be predicted without using a turbulence model, even though significant fluctuations may be present. In practice, information needed to use this definition is available only from measurements of velocity profiles. Moller[12] has measured exit-velocity distributions for source flow between stationary discs for a range of local Reynolds number Re. His data begin to deviate from a turbulent power-law profile for $Re=5250$ and 3050, while it can be fitted by a parabola for $Re=1000$ and 1300, indicating that reverse transition occurs, roughly, over the range $5000\geqslant Re\geqslant 1000$.

The influence of reverse transition is included by introducing an 'intermittency' γ which multiplies the eddy viscosity for tmi. This intermittency is unity for fully-turbulent flow and decreases as Re decreases according to a form suggested by an empirical correlation for the decay of turbulent kinetic energy in reverse transition[9]. If reverse transition is assumed to begin at $R=R_{cr}$ where $Re=Re_{cr}$ and continues until the flow is essentially laminar at $Re=Re_{lam}$, the intermittency is, for $Re\leqslant Re_{cr}$:

$$\gamma=\exp\left[-c(Re_{cr}-Re)^3\left(\frac{1}{Re}-\frac{1}{Re_{cr}}\right)\right]. \tag{16}$$

The empirical constant c is specified by requiring that $\gamma = \exp(-3)$ at $Re = Re_{lam}$. From Moller's data discussed above, $Re_{cr} = 5000$ and $Re_{lam} = 1000$ were chosen.

Solution method

A sequence of related parabolic problems for which only a numerical solution is practical has been established. The Box method[15] was chosen because its generality makes it readily adaptable to new situations; it provides both a method for establishing the appropriate difference equations and a solution method. The key to the method is reformulation of the governing equations as a system of first-order equations. Thus the second derivatives which appear due to the cross-stream diffusion terms require the introduction of additional unknown functions:

$$S = \frac{\partial U}{\partial Z} \tag{17a}$$

$$T = \frac{\partial V}{\partial Z} \tag{17b}$$

The momentum equations which result from the use of Eq (8) in Eqs (5) and (6) are then transformed to a system of five first-order equations:

$$F' = U \tag{18a}$$

$$U' = S \tag{18b}$$

$$V' = T \tag{18c}$$

$$R[(1+\varepsilon_R^+)S]' = \frac{-U^2}{R} - \left(\frac{Re_\omega}{Re_s}\right)^2 R^3 V^2 + U\frac{\partial U}{\partial R} - \frac{\partial F}{\partial R}S + R^2\frac{dP}{dR} \tag{18d}$$

$$R[(1+\varepsilon_\theta^+)T]' = \frac{2UV}{R} + U\frac{\partial V}{\partial R} - \frac{\partial F}{\partial R}T \tag{18e}$$

where prime denotes partial differentiation with respect to Z.

The boundary conditions can be expressed in a form that is consistent with Eqs (18) using Eqs (8) and (17) to obtain:

$$F(R,0) = 0 \tag{19a}$$

$$U(R,0) = 0 \tag{19b}$$

$$V(R,0) = 1 \tag{19c}$$

$$F(R,Z_c) = Z_c \tag{19d}$$

$$S(R,Z_c) = 0 \tag{19e}$$

$$T(R,Z_c) = 0 \tag{19f}$$

With no loss of generality, $F(R,0) = 0$ was chosen. Even though the turbulence models do not require any additional starting information, starting conditions must be specified for all dependent variables because the Box method uses two-point averages in the streamwise direction. The determination of these starting conditions at $R = R_s$ is discussed below. The choice for pressure at $R = R_s$ is arbitrary.

The complete system of non-linear difference equations is solved iteratively by Newton's method at each radial station. Following usual practice[15], ε_R^+ and ε_θ^+ are lagged during this process, ie their values for the i iteration are used in the $(i+1)$ iteration. Experience has shown that the wall shear stress is a sensitive indicator of convergence[15]. Hence the convergence criterion for the inner iterations required that successive values of S evaluated at the wall change by less than 0.1%. The pressure gradient was determined by an outer iteration[26] using the boundary condition given as Eq (19d). The linear system solved within each Newton iteration has a special block-tridiagonal form which permits an efficient solution. This form was obtained in a manner similar to the usual two-dimensional formulation[28]. Some additional, but straightforward, algebraic manipulation was required to treat the 5×5 matrices which result from Eq (18). The difference and matrix equations are listed elsewhere[16].

Starting conditions at R_s are determined by a local-similarity[17] approximation to Eqs (18) in which the radial variation of F, S, T, U and V is ignored. The solution procedure is identical to that followed at each radial step in the marching solution, including the simultaneous determination of the pressure gradient. Initial estimates for the dependent variables and turbulence quantities for the iteration within the local-similarity solution were determined from arbitrarily specified velocity distributions; parabolic or power-law profiles were adequate. A partial example of the computed starting conditions is shown in Fig. 6.

Since starting conditions based on local similarity are only approximate solutions of the governing equations, oscillations between marching steps appear in the computed solution. Cebeci[29] recommends the use of small marching steps near R_s and a smoothing procedure to remove these oscillations. Computations begin at $R = R_s$, and marching steps are taken to $R = R_s + \Delta R$ and $R = R_s + 2\Delta R$. Averaging between adjacent radial stations provides distributions of all variables at $R = R_s + (1/2)\Delta R$ and $R = R_s + (3/2)\Delta R$. These two distributions are then averaged to obtain new, 'smoothed' profiles at $R = R_s + \Delta R$. The second-order accuracy of the method is retained in this averaging procedure[30]. Approximately ten marching steps with small ΔR are taken in the starting region. These initial steps are typically $\Delta R = 0.01\, R_s$, and the step size is then gradually increased; it can be as large as $\Delta R = R_s$ at large radius, eg at $R = 10R_s$. A variable axial grid spacing as suggested by Keller and Cebeci[15] was employed. Approximately twenty axial grid points provide 1% accuracy.

The numerical procedure is very efficient with only modest core storage requirements. The code was executed on an IBM 3032/4341 system, with computation times of the order of one second per radial station. Typically two inner iterations within each of five outer iterations were required in each radial marching step. The difference in computation time for various flow cases or turbulence models are insignificant.

Results

To test the computer implementation of the turbulence modelling and solution method, two previously studied flows were examined. In the first, turbulent developing flow in the entrance of a parallel-plate duct[26], good agreement with the earlier work was achieved. Since the numerical procedure can easily treat laminar flows as a special case, the general computer code was next used to

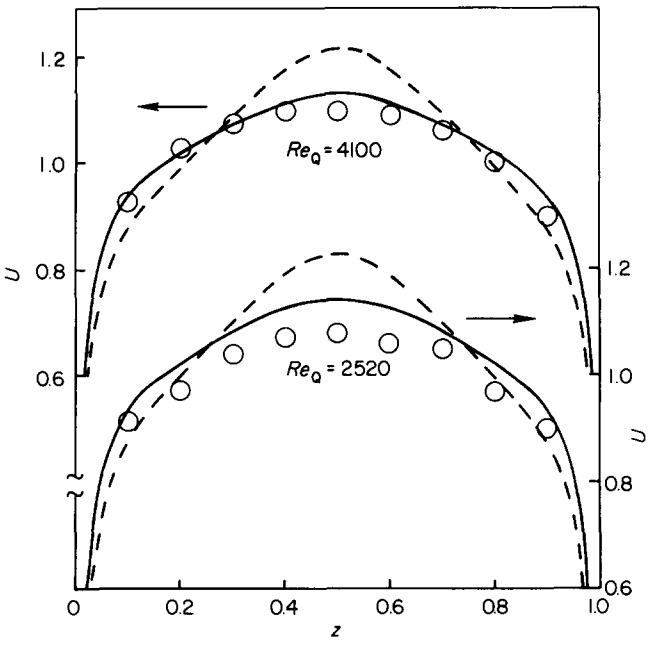

Fig 1 Comparison of predictions of U (*solid line – tmi; dashed line – tmi with* $\alpha=0.0$) *and data* (○ *Bayley and Owen*[10]) *at exit radius* ($R/R_s=3.125$, $r_s/h=10.67$) *for stationary discs*

solve the problem of laminar source flow for both stationary and rotating discs. The results obtained are also in good agreement with earlier work[6].

Several sets of data for turbulent source flow between stationary discs appear in the literature. Measurements of the radial static-pressure distribution were made by Moller[12], Bayley and Owen[10] and Bakke *et al*[13]. Moller and Bayley and Owen also determined the axial distribution of radial velocity at the exit of the discs using a pitot tube. Bakke *et al* completed several axial traverses for radial velocity at various radial locations using a hot-wire anemometer.

The data of Bayley and Owen and some of Moller's data are at Reynolds numbers large enough that reverse-transition effects should not be significant. In each case the accuracy of the pitot-tube measurement is unknown because no uncertainty is given. The effect of the exit region upon these measurements at the outer radius is also unknown. Nevertheless, these data represent the only test of the constants in the turbulence model tmi. Predictions using tmi are compared with the data of Bayley and Owen in Fig 1. For $\alpha=0$, which eliminates the Bradshaw modification[5] for extra strain rate, the agreement is poor. An important conclusion is that this modification should be included in the turbulence modelling. Examination of the sensitivity of predictions using tmi to variations in the empirical constants[16] shows them to be quite insensitive to changes in κ and A^+ while the values for λ and α are more important. The choices for the constants in tmi appear to be reasonable although they are probably not optimum.

Bakke *et al* present velocity distributions for five different cases of source flow between stationary discs. Measurements were made by inserting a hot-wire probe into the flow region between the discs and the influence of obstruction by this probe is unknown, but it is likely significant. Evidence for this conclusion is provided by Nguyen, Ribault and Florent[31], who, for laminar flow between a fixed disc and a rotating disc, show a large dependence of their experimental results on the anemometry technique used. The finite size of any probe also makes it difficult to obtain data near a wall and heat-transfer effects between the probe and the disc surface change the nonlinear calibration of the probe. At the measuring location nearest the disc, velocities of 0.3 m/s (1 ft/s) were measured by Bakke *et al* even with no source flow. The 'no-flow' readings were subtracted from the measurements with source flow to account for this error. Thus Bakke *et al* suggested that velocity measurements within 0.038 cm (0.015 in) of the disc surface have considerable error. Therefore their data are not reliable for $Z/Z_c<0.15$ for $r_s/h=9.050$ and for $Z/Z_c<0.10$ for $r_s/h=6.033$. This explains some of the unusual behaviour in the velocity distributions near the disc surface. For emphasis, these unreliable data are denoted by solid symbols in the pertinent figures.

An additional feature of the apparatus used by Bakke *et al* is apparent in the measured velocity distributions. Because the axial inlet flow at the centre of their horizontal discs was introduced from only the bottom, a strong asymmetry extended, in some cases, over a significant portion of the flow region. Obviously such results cannot be compared to our predictions which assume a symmetric velocity profile.

In spite of these difficulties, the overall scarcity of pertinent data makes it worthwhile to attempt to draw some useful information from the data of Bakke *et al*. However, since Re at the exit for this data lies in the range $1000<Re<3000$, the effects of reverse transition should be included. Predictions for source flow between stationary discs with and without reverse transition are compared with the measurements of Bakke *et al* in Fig 2; in Fig 2(c), Re is large enough that γ is nearly one and the results with and without intermittency are indistinguishable in the scale of the figure. Omitting the region near the wall where the data is not reliable, the agreement with the predictions which include reverse transition is satisfactory. The predictions correctly follow the behaviour of the data with increasing effects of reverse transition at smaller Re. This agreement is, at least, indirect evidence that the turbulence modelling embodied in tmi is an adequate basis for engineering studies of turbulent source flow between stationary discs.

The data of Bakke *et al* for the radial velocity component are normalized by the centre line values; since these values are not available, it is not possible to make more precise comparisons. Tabulated values of $U(R,Z_c)$ for our predictions are available from the authors upon request.

An extensive set of measurements for turbulent source flow between rotating discs was presented by Bakke *et al*. Their measurements for flow between rotating discs are subject to the same limitations as the measurements for stationary discs discussed earlier. Predictions for three typical cases which span the range of the data of Bakke *et al* are compared with measurements in Fig 3. As expected, in the case with the smallest Re_ω (Fig 3(a)), anisotropic effects are least important; even the isotropic predictions (tmi) are reasonable. As Re_ω increases with ω (Fig 3(b)) or h (Fig 3(c)), the anisotropic predictions using tma more nearly predict the shape of the measured distributions. The predictions of tangential

velocity and pressure are relatively insensitive to the turbulence model as shown in Figs 4 and 5. The pressure distribution does not reflect local conditions and is not, by itself, an adequate test of the turbulence modelling. Bakke *et al*, in fact, obtained good agreement for pressure using an integral method. Truman[16] shows that the empirical constants chosen earlier remain reasonable for rotating discs.

Because the parameter ranges for the data are limited, a series of predictions over a larger range of the flow parameters was made. The parameter ranges for these predictions were: $Re_Q = 200$ to 5000; $Re_\omega = 100$, 200 and 500, and $r_s/h = 5$, 10 and 20. The values of Re_Q were chosen to be large enough that reverse-transition effects should be unimportant. This conclusion is consistent with the experimental transition results of Pater *et al*[8]. Moreover, the experimental results of Bakke *et al* show that, in general, turbulence intensities increase with radius, indicating that rotation eliminates, or at least delays, reverse transition. The ranges of Re_ω and spacing ratio r_s/h include the available data and extend to larger values. These predictions are sufficient to demonstrate trends in the flow behaviour with variations in the parameters.

The flow behaviour with increasing radius is similar when the ratio Re_Q/Re_ω and the spacing ratio r_s/h are held constant; this is a result of the definition of the dimensionless radius R. For small Re_Q/Re_ω as in Fig 6, the effects of rotation become significant as R increases. In fact, for $R/R_s > 7$, the flow reversal mentioned earlier ($U(R,Z_c) < 0$) occurs and the parabolic model is invalid. When Re_Q/Re_ω is large, however, the effects of rotation are not very important even for $R/R_s = 10$. Fig 6 also shows that, when Re_Q/Re_ω, r_s/h and R/R_s are duplicated, the results are approximately the same regardless of the actual values of Re_Q and Re_ω. This might provide a basis for estimating *a priori* the occurrence of flow reversal. The effect of varying r_s/h, which is significant only for small Re_Q/Re_ω, is shown in Fig 7. Similarly the effect of varying Re_Q/Re_ω is important only for small r_s/h. Details are given elsewhere[16].

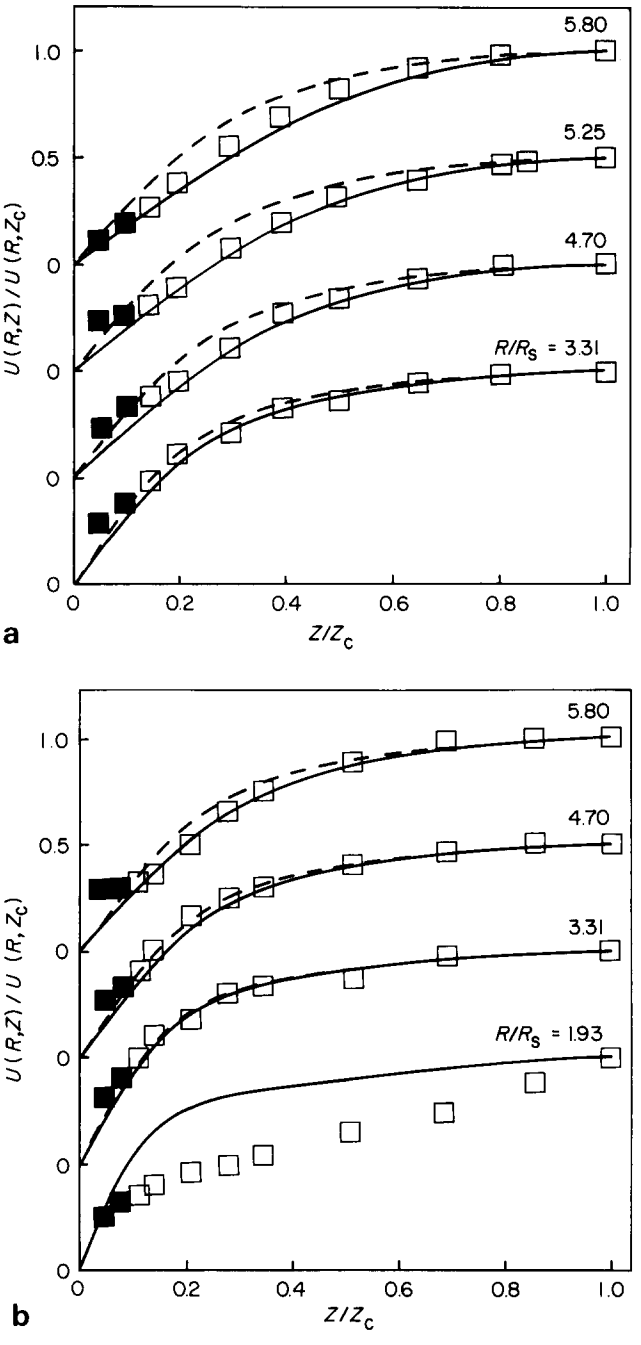

Fig 2 Comparison of predictions of U(R,Z)/U(R,Z_c) *(solid line – tmi with γ; dashed line – tmi without γ) and data (□ Bakke[13]) at several radial positions* (R/R_s) *for stationary discs. Solid symbols denote unreliable data.*
(a) $Re_Q = 379.5$, $r_s/h = 9.050$, $1180 < Re < 2070$;
(b) $Re_Q = 857.5$, $r_s/h = 6.033$, $1780 < Re < 5350$;
(c) $Re_Q = 850.7$, $r_s/h = 9.050$, $2660 < Re < 7960$

Conclusions

Engineering predictions for turbulent source flow between stationary and corotating parallel discs have been presented. The predictions for the rotating case are the first local results available and the results for the stationary case extend earlier work substantially, particularly with the inclusion of the Bradshaw modification[5] for the extra strain rate caused by stream-

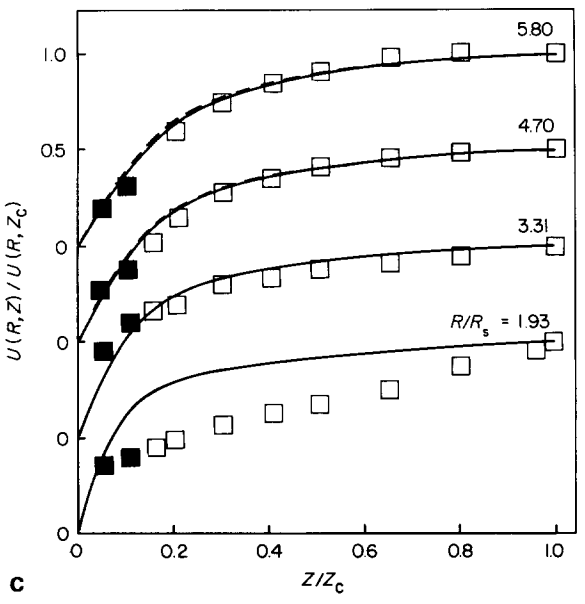

line divergence and the intermittency factor for reverse transition. Comparisons with data have been made where possible. Optimization of the turbulence models was not possible because of the inadequacy and scarcity of pertinent experimental information. However, the turbulence models provide reasonable results when the empirical constants are selected by examination of similar flows. This conclusion seems to justify the original decision to treat the flow as a perturbation of a classical thin shear layer.

The extra strain rate due to streamline divergence

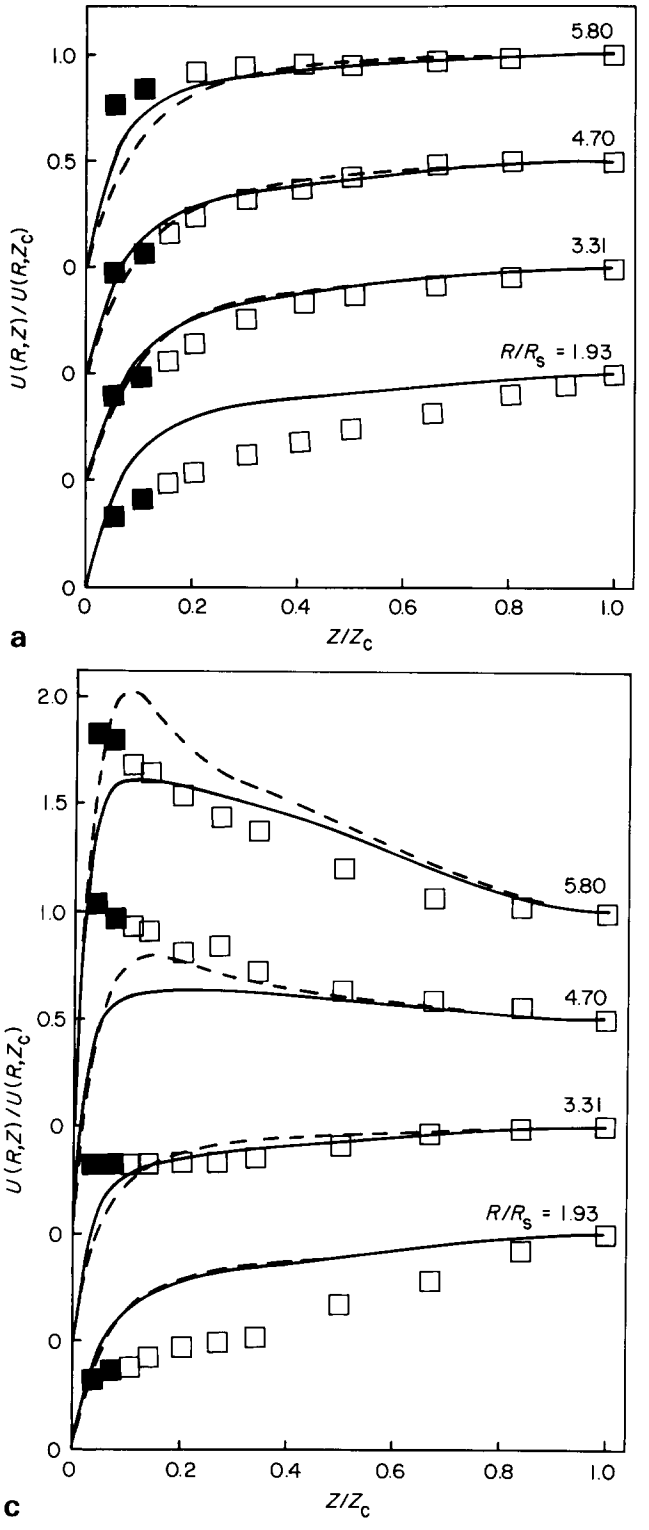

Fig 3 Comparison of predictions of U(R,Z)/U(R,Z_c) *(solid line – tmi; dashed line – tma) and data (□ Bakke* et al[13]*) at several radial positions* (R/R_s) *for rotating discs. Solid symbols denote unreliable data.*
(a) $R_Q = 850.7$, $Re_\omega = 110.9$, $r_s/h = 9.050$;
(b) $Re_Q = 850.7$, $Re_\omega = 221.6$, $r_s/h = 9.050$;
(c) $Re_Q = 1276$, $Re_\omega = 500.9$, $r_s/h = 6.033$

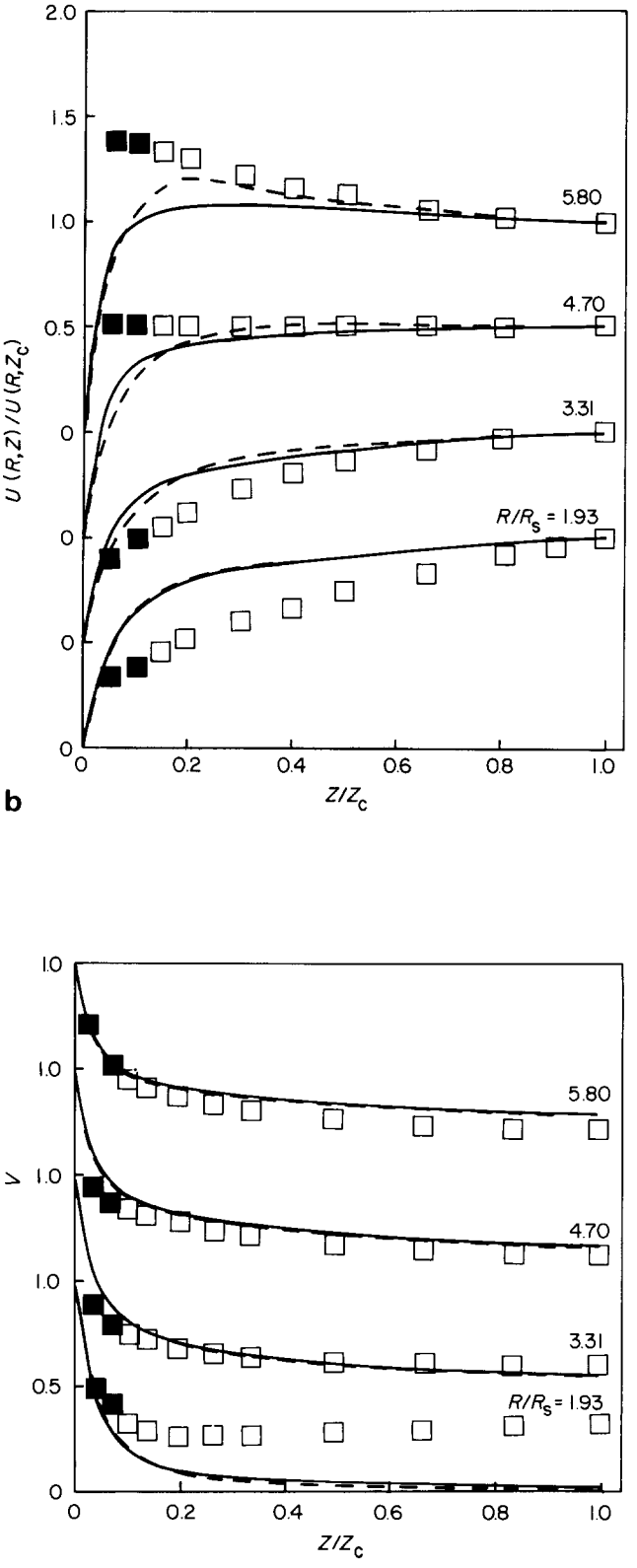

Fig 4 Comparison of predictions of V *(solid line – tmi; dashed line – tma) and data (□ Bakke* et al[13]*) at several radial positions* (R/R_s) *for* $Re_Q = 1276$, $Re_\omega = 500.9$ *and* $r_s/h = 6.033$. *Solid symbols denote unreliable data*

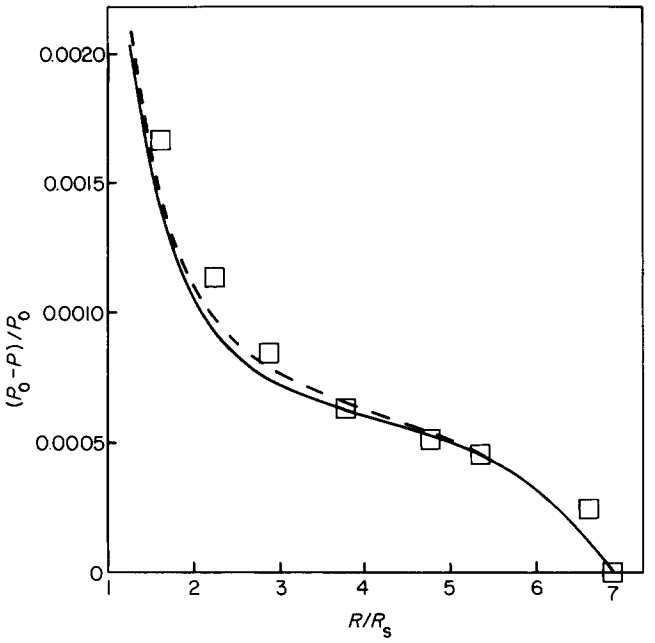

Fig 5 Comparison of predictions of $(P_0 - P)/P_0$ *(solid line – tmi; dashed line – tma) and data (□ Bakke* et al[13]*) for* $Re_Q = 1276$, $Re_\omega = 500.9$ *and* $r_s/h = 6.033$

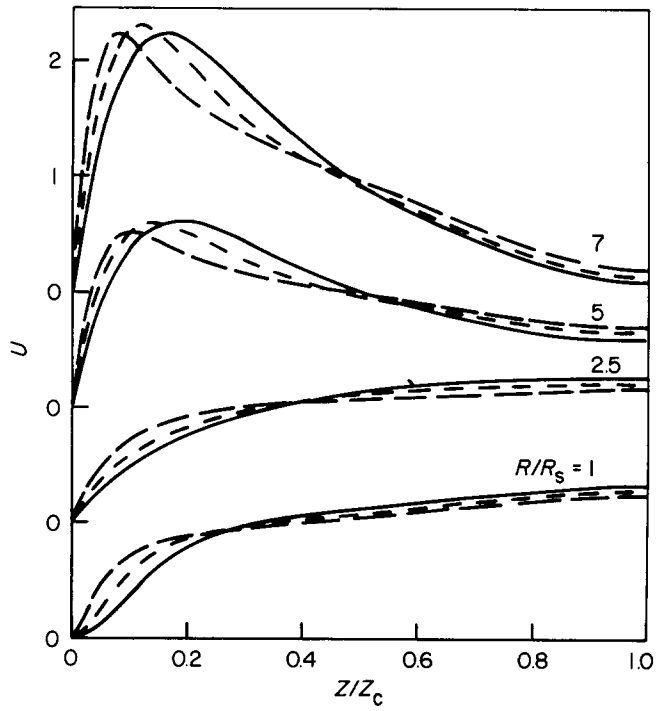

Fig 6 Predictions (tma) of U *at several radial positions* (R/R_s) *for* $Re_Q/Re_\omega = 2$ *and* $r_s/h = 5$ (—— $Re_Q = 200$; – – – $Re_Q = 400$; ———— $Re_Q = 1000$)

was shown to have a significant effect, which is successfully modelled by including the simple Bradshaw modification in the turbulence models. The effects of disc rotation required an anisotropic turbulence model; reasonable success was achieved with turbulence model tma. A formula for treating reverse transition was developed. While this result is completely empirical, its use does extend the range of flow cases that can be treated reasonably.

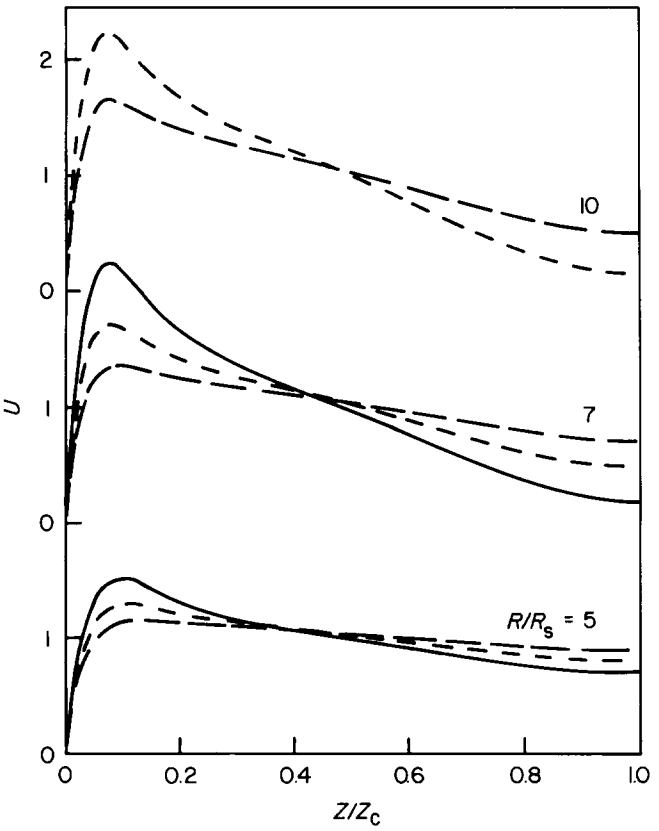

Fig 7 Predictions (tma) of U *at several radial positions* (R/R_s) *for* $Re_Q = 1000$ *and* $Re_\omega = 500$ *for various* r_s/h (—— $r_s/h = 5$; – – – $r_s/h = 10$; ———— $r_s/h = 20$)

Until more extensive and reliable empirical information is available, significant improvements over the present results in the prediction of turbulent source flow between parallel discs are not likely. With such information, the present models can be improved, or more sophisticated turbulence models, such as the $k-\varepsilon$ model, can be used, to provide higher-quality predictions.

Acknowledgments

Professors P. Bradshaw and T. Cebeci kindly responded to questions regarding turbulence modelling and numerical-solution procedures. This work was supported in part (C.R.T.) by an Arizona State University Dissertation-Year Fellowship and by Sandia National Laboratories – Albuquerque.

References

1. **Paivanas J. A. and Hassan J. K.** Attraction force characteristics engendered by bounded, radially diverging air flow. *IBM J. Res. Dev. 1981*, **25**, *176–186*
2. **Bogy D. B., Fromm J. E. and Talke F. E.** Exit region central source flow between finite closely spaced parallel corotating discs. *Phys. Fluids, 1977*, **20**, *176–186*
3. **Lenneman E.** Aerodynamic aspects of disc files. *IBM J. Res. Dev., 1974*, **18**, *480–488*
4. **Felsch K. O. and Piesche M.** Calculation of the flow through an element of a shear-force pump with temperature-dependent viscosity for the transfer of highly-viscous fluids (in German). *Acta Mech., 1981*, **38**, *19–30*

5. **Bradshaw P.** Review: Complex turbulent flows. *ASME J. Fluids Eng., 1975*, **97**, *146–154*

6. **Boyd K. E. and Rice W.** Laminar inward flow of an incompressible fluid between rotating discs with full peripheral admission. *ASME J. Appl. Mech., 1968*, **35**, *229–237*

7. **Adams R. G. and Rice W.** Experimental investigation of the flow between corotating discs. *ASME J. Appl. Mech., 1970*, **37**, *844–849*

8. **Pater L. L., Crowther E. and Rice W.** Flow regime definition for flow between corotating discs. *ASME J. Fluids Eng., 1974*, **96**, *29–34*

9. **Narasimha R. and Sreenivasan K. R.** Relaminarization of fluid flows. *Adv. Appl. Mech., 1979*, **19**, *221–307*

10. **Bayley F. J.** and **Owen J. M.** Flow between a rotating and a stationary disc. *Aeronaut. Q., 1969*, **20**, *333–354*

11. **Murphy H. D., Chambers F. W. and McEligot D. M.** Laterally converging flow. Part 1. Mean flow. *J. Fluid Mech., 1983*, **127**, *379–401*

12. **Moller P. S.** Radial flow without swirl between parallel discs. *Aeronaut. Q., 1963*, **14**, *163–186*

13. **Bakke E., Kreider J. F. and Kreith F.** Turbulent source flow between parallel stationary and co-rotating discs. *J. Fluid Mech., 1973*, **58**, *209–231*

14. **Koosinlin M. L. and Lockwood F. C.** The prediction of axisymmetric turbulent swirling boundary layers. *A.I.A.A. J., 1974*, **12**, *547–554*

15. **Keller H. B. and Cebeci T.** Accurate numerical methods for boundary-layer flows. II: Two-dimensional turbulent flows. *A.I.A.A. J., 1972*, **10**, *1193–1199*

16. **Truman C. R.** *Ph.D. thesis, Arizona State University, 1983 (available from University Microfilms, order no. DA8322535)*

17. **Sparrow E. M., Quack H. and Boerner C. J.** Local nonsimilarity boundary-layer solutions. *A.I.A.A. J., 1970*, **8**, *1936–1942*

18. **Launder B. E., Priddin C. H. and Sharma B. I.** The calculation of turbulent boundary layers on spinning and curved surfaces. *ASME J. Fluids Eng., 1977*, **99**, *231–239*

19. **Sharma B. I.** Prediction of mass transfer near a rotating disc at high Schmidt numbers and high swirl rates. *Int. J. Heat Mass Transfer, 1978*, **21**, *1355–1356*

20. **Cebeci T. and Abott D. E.** Boundary layers on a rotating disk. *A.I.A.A. J., 1975*, **13**, *829–832*

21. **Cooper P. and Reshotko E.** Turbulent flow between a rotating disk and a parallel wall. *A.I.A.A. J., 1975*, **13**, *573–578*

22. **Koosinlin M. L., Launder B. E. and Sharma B. I.** Prediction of momentum, heat and mass transfer in swirling, turbulent boundary layers. *ASME J. Heat Transfer, 1974*, **96**, *204–209*

23. **Smits A. J., Eaton J. A. and Bradshaw P.** The response of a turbulent boundary layer to lateral divergence. *J. Fluid Mech., 1979*, **94**, *243–268*

24. **Rodi W.** Turbulence models and their applications in hydraulics. *State-of-the-Art Paper, Int. Assoc. for Hydraulic Research, Delft, The Netherlands, 1980*

25. **Dean R. B.** *Ph.D. thesis, University of London, Imperial College, 1974*

26. **Cebeci T. and Chang K. C.** A general method for calculating momentum and heat transfer in laminar and turbulent duct flows. *Numer. Heat Transfer, 1978*, **1**, *39–68*

27. **Rotta J. C.** A family of turbulence models for three-dimensional boundary layers. in *Turbulent Shear Flows I, (eds. F. Durst, B. E. Launder, F. W. Schmidt and J. H. Whitelaw), Springer-Verlag, 1979, 267–278*

28. **Cebeci T. and Bradshaw P.** Momentum transfer in boundary layers. *Hemisphere, 1977*

29. **Cebeci T.** *Personal communication, 1982*

30. **Keller H. B.** Some computational problems in boundary-layer flows. *Proc. Fourth Int. Conf. on Numerical Methods in Fluid Dynamics, Lecture Notes in Physics, 1975*, **35**, *1–21*

31. **Nguyen N. D., Ribault J. P. and Florent P.** Multiple solutions for flow between coaxial discs. *J. Fluid Mech., 1975*, **68**, *369–388*